

# Coexistence of two different energy transfer processes in SiO<sub>2</sub> films containing Si nanocrystals and Er

Minoru Fujii,<sup>a)</sup> Kenji Imakita, Kei Watanabe, and Shinji Hayashi

*Department of Electrical and Electronics Engineering, Faculty of Engineering, Kobe University, Rokkodai, Nada, Kobe 657-8501, Japan*

(Received 3 July 2003; accepted 14 October 2003)

The mechanism of energy transfer from silicon nanocrystals (nc-Si) to erbium ions (Er<sup>3+</sup>) in SiO<sub>2</sub> films containing nc-Si and Er was studied by analyzing delayed infrared luminescence from Er<sup>3+</sup>. It was found that, to theoretically reproduce the rising part of the time-dependent luminescence intensity, two different energy transfer processes, i.e., fast and slow processes, should be considered. From the fitting of the delayed luminescence to a model, the ratio of the two energy transfer processes and the energy transfer rate of the slow process were estimated. The ratio exhibited a clear dependence on the luminescence peak energy of Si nanocrystals, which act as photosensitizers for Er<sup>3+</sup>, indicating that the ratio depends on the size of nc-Si. The ratio of slow to fast processes increased with the decrease in size; this observation is a strong indication that the fast process is the direct inheritance of the process in bulk Si:Er systems, and the slow process is a characteristic process occurring only in nc-Si:Er systems. The energy transfer rate of the slow process was found to depend on the recombination rate of excitons in nc-Si. © 2004 American Institute of Physics. [DOI: 10.1063/1.1631072]

## I. INTRODUCTION

The electronic structure of silicon nanocrystals (nc-Si) is strongly modified from that of bulk Si crystals due to the confinement of electrons and holes in a space smaller than the exciton Bohr radius of bulk Si crystals.<sup>1,2</sup> The modification of the electronic structure provides nc-Si with functions which do not occur in bulk Si crystals. For example, one function is as a photosensitizer for optically inactive materials. Recently, nc-Si were demonstrated to act as photosensitizers for molecular oxygen<sup>3,4</sup> and several kinds of rare earth ions.<sup>5–18</sup> In particular, erbium ions (Er<sup>3+</sup>) can be excited very efficiently by the energy transfer from nc-Si; the effective absorption cross section of the intra-4*f* shell transition of Er<sup>3+</sup> is enhanced by 2–4 orders of magnitude because of the large absorption cross section of nc-Si in a visible range and because of the efficient energy transfer from nc-Si to Er<sup>3+</sup>.<sup>5–15</sup> This sensitized excitation of Er<sup>3+</sup> provides large benefits in a number of fields which utilize near-infrared emission of Er<sup>3+</sup>. One application which takes advantage of the enhanced absorption cross section is a planar-waveguide optical amplifier operating at 1.54 μm. With a simple ridge-type waveguide structure (1 cm long, 9 μm wide, and 0.5 μm high) consisting of SiO<sub>2</sub> films containing nc-Si and Er excited from the top, a net gain of 7 dB/cm at 1.535 μm has been obtained.<sup>19,20</sup> By employing similar materials as a gate oxide of a metal–oxide–semiconductor structure, electroluminescence devices operating at room temperature with the quantum efficiency of 1%<sup>21</sup> and 10%<sup>22</sup> have been reported.

Because of these possible applications, great efforts have been devoted to understanding the mechanism of the inter-

action between nc-Si and Er<sup>3+</sup>. One standard approach in analyzing the interaction is to construct a set of rate equations by taking into account all possible transitions in and between nc-Si and Er<sup>3+</sup>, fitting the experimental data to the model, and extracting parameters describing the energy exchange processes. This approach has worked very well, and all experimental results have been explained consistently.<sup>16</sup> Furthermore, by extending this approach, a guideline to realizing an optical amplifier from nc-Si:Er systems has been given.<sup>16</sup>

In these previous studies, the coupling between nc-Si and Er is assumed to be very strong. However, this assumption is not always applicable. In our previous work on SiO<sub>2</sub> films containing nc-Si and Er,<sup>14</sup> we demonstrated that, after excitation of nc-Si by a pulse laser with a 5 ns pulse width, the photoluminescence (PL) intensity of Er<sup>3+</sup> rises very fast up to about 70% of the maximum intensity, and then starts to rise slowly until reaching the maximum. The observed delay time was distributed from several microseconds to several hundredths of a microsecond, depending on the sample preparation conditions. The observation of the long PL delay suggests that, in addition to the strong coupling that is usually considered, a weak coupling process exists, although it might play a minor part in the whole energy transfer process.

Another point not discussed in detail so far is the size dependence of the interaction properties. In previous models, nc-Si:Er systems have been treated as an independent system that is essentially different from Er-doped bulk Si (bulk-Si:Er) systems, that is, no continuity from bulk-Si:Er to nc-Si:Er systems has been discussed. This distinction seems to be reasonable by considering different exciton transport properties between the two systems; in nc-Si:Er systems, excitons can interact only with Er<sup>3+</sup> staying nearby each nanocrystal, while in bulk-Si:Er systems, excitons can migrate

<sup>a)</sup> Author to whom correspondence should be addressed; electronic mail: fujii@eedept.kobe-u.ac.jp

and interact with any  $\text{Er}^{3+}$ . However, it is not plausible that the mechanism of the energy-exchange itself is completely different between the two systems. The electronic structure of nc-Si is modified only slightly from that of bulk Si crystals, and the electronic structure changes continuously from the bulk structure with decreasing size.<sup>1,2</sup> As a result, the optical property of nc-Si is a small modification of those of bulk Si crystals, and all parameters (e.g., band gap energy, exciton lifetime, degree of electron-hole exchange interaction, and so on) change continuously from the bulk values. It is well-established from experimental and theoretical studies that all these changes are the results of spatial confinement of electrons and holes, or excitons in a small space (i.e., the quantum size effect).<sup>1,2</sup> The exciton Bohr radius of a bulk Si crystal is about 5 nm. The quantum size effect thus becomes prominent for nanocrystals smaller than about 10 nm in diameter, and larger nanocrystals can be regarded as bulk from the point of view of electronic structures. Therefore, if the strong interaction between nc-Si and  $\text{Er}^{3+}$  is a consequence of quantum size effects, we should observe continuous changes of the interaction properties from bulk-Si:Er-like to nc-Si:Er-like in the size range less than 10 nm.

The purpose of this work is to have experimental access to these problems. To do so, we extended our previous work on  $\text{SiO}_2$  films containing nc-Si and Er.<sup>14</sup> We have studied the time development of  $\text{Er}^{3+}$  PL intensity after pulsed excitation of nc-Si hosts. The rising part of  $\text{Er}^{3+}$  PL intensity contains valuable information concerning the energy transfer mechanism. We will demonstrate that, in order to quantitatively reproduce the observed rising part, two different energy transfer processes (fast and slow) should be considered. From the fitting of observed curves to a model, the ratio of the two processes and the energy transfer rate of the slow process are extracted. It will be shown that the ratio depends greatly on the size of nc-Si and changes continuously in a wide size range; this continuous change indicates that there is no distinct border from bulk Si to nc-Si in the sense of energy exchange with  $\text{Er}^{3+}$ . The observed size dependence implies that the slow energy transfer process is a characteristic process occurring only in nc-Si:Er systems, thus becoming more important with decreasing size. It will be shown that the energy transfer rate of the slow process is determined by the recombination rate of excitons in nc-Si.

## II. EXPERIMENTAL DETAILS

$\text{SiO}_2$  films containing nc-Si and Er ( $\text{SiO}_2$ :nc-Si:Er) were prepared by a cosputtering method. Details of the preparation procedures are described in our previous papers.<sup>6,7</sup> Si,  $\text{SiO}_2$ , and  $\text{Er}_2\text{O}_3$  were simultaneously sputter deposited in argon (Ar) gas, and the deposited films (about 1  $\mu\text{m}$  in thickness) were annealed in a nitrogen ( $\text{N}_2$ ) gas (99.999%) atmosphere for 30 min at temperatures between 1100 and 1250 °C. Si nanocrystals were grown in films of the mixture of  $\text{SiO}_2$  and  $\text{Er}_2\text{O}_3$  during the annealing. In this method, the size of nc-Si can be controlled by changing the concentration of Si in the films or changing the annealing temperature. The average size of nc-Si was estimated by cross-sectional transmission electron microscopic observa-

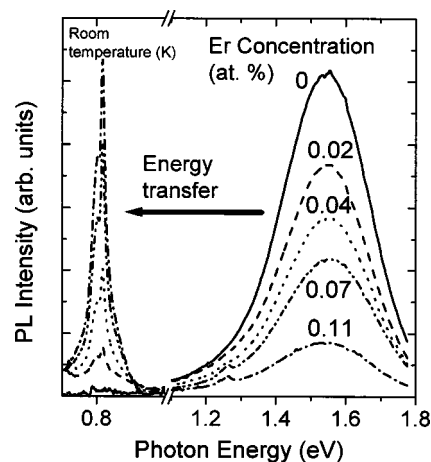


FIG. 1. Photoluminescence spectra of  $\text{SiO}_2$  films containing Si nanocrystals and Er at room temperature. A broadband at about 1.55 eV is due to recombination of excitons in Si nanocrystals and a sharp peak at 0.81 eV arises from intra-4*f* shell transition of  $\text{Er}^{3+}$ .

tions. In this work, the average size of nc-Si ( $d_{\text{Si}}$ ) was changed from 2.7 to 5.5 nm. Er concentration was fixed to 0.11 at.% for all the samples. PL spectra were measured using a single grating monochromator and a near-infrared photomultiplier with an InP/InGaAs photocathode. The excitation source for taking the spectra was the 457.9 nm line of an Ar-ion laser (0.3 W/cm<sup>2</sup>). In this wavelength,  $\text{Er}^{3+}$  is not directly excited. For all the spectra, the spectral response of the detection system was corrected by the reference spectrum of a standard tungsten lamp. For the time response measurements, a 532.0 nm line of a Nd:Yttrium–aluminum–garnet (YAG) laser was used as the excitation source (pulse energy 0.65 mJ, pulse width 5 ns, repetition frequency 20 Hz, and spot size 2 mm). A multichannel scalar was used in obtaining the decay curves. The overall time resolution of the system was better than 100 ns. All measurements were performed at room temperature.

## III. RESULTS AND DISCUSSION

### A. Analysis of PL decay curves

Figure 1 shows the typical PL spectra of  $\text{SiO}_2$  films containing Si nanocrystals and Er at relatively low Er concentration ranges ( $\sim 0.11$  at.%). Two emission bands due to the exciton recombination in nc-Si and intra-4*f* shell transition of  $\text{Er}^{3+}$  are observed. The intensities of these bands compete with each other; with increasing Er concentration, the  $\text{Er}^{3+}$  PL band becomes stronger, while the exciton PL band is quenched. The ratio of the increase in  $\text{Er}^{3+}$  PL intensity (integrated intensity) to the loss of nc-Si PL one was about 0.7 at low excitation power. The excitation spectrum of the  $\text{Er}^{3+}$  PL is very similar to that of the exciton PL, indicating that excitation of  $\text{Er}^{3+}$  is due mainly to the energy transfer from Si nanocrystals.<sup>7</sup>

More evidence of the energy transfer is obtained in the time transient of  $\text{Er}^{3+}$  PL.<sup>14</sup> Figure 2 shows the time dependence of PL intensity just after excitation by the frequency-doubled pulsed Nd:YAG laser with a pulse width of 5 ns. The time resolution of the detection system is better than 100

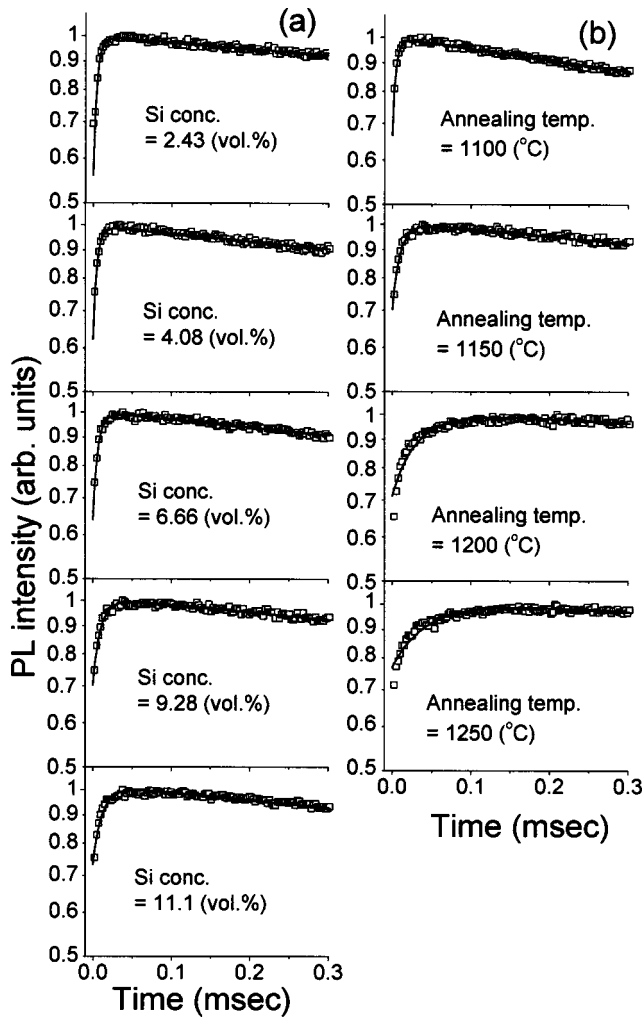


FIG. 2. PL time transient at 0.81 eV just after 5 ns pulsed excitation. Symbols are experimental results, and curves are results of model fittings. (a) Annealing temperature and Er concentration are fixed at 1150 °C and 0.11 at. %, respectively, and excess Si concentration is changed. (b) Excess Si concentration and Er concentration are fixed at 9.28 vol % and 0.11 at. %, and annealing temperature is changed.

ns. We can clearly see that PL intensity rises slowly after finishing the excitation, and the delay time depends strongly on the samples. The observation of the delayed PL is the direct evidence that  $\text{Er}^{3+}$  is excited indirectly by the energy transfer from nc-Si.

It is worth noting that, although excitation of  $\text{Er}^{3+}$  is due mainly to the energy transfer, at the present excitation wavelength (532 nm), the direct excitation of  $\text{Er}^{3+}$  is also partially possible. In order to know the extent of the contribution of direct excitation, we compared PL intensities of the present samples to other samples without nc-Si but with the same amount of  $\text{Er}^{3+}$  ( $\text{SiO}_2:\text{Er}$ ). The PL intensity obtained for the  $\text{SiO}_2:\text{Er}$  samples was less than 5% of the PL intensity of the  $\text{SiO}_2:\text{nc-Si}:\text{Er}$  samples, suggesting that the contribution of direct excitation is negligibly small in  $\text{SiO}_2:\text{nc-Si}:\text{Er}$  samples.

In the present sample preparation method, the size of nc-Si can be controlled by two independent parameters, i.e., excess Si concentration and annealing temperature. In Fig. 2(a), the Er concentration (0.11 at. %) and annealing tem-

perature (1150 °C) are fixed and the excess Si concentration is changed. By changing the excess Si concentration from 2.43 to 11.1 vol %, the PL peak energy is shifted from 1.52 to 1.36 eV (see Table I), corresponding to the size change of 3.2–4.6 nm. We can see that with increasing the size, the PL delay becomes slightly longer. In contrast to Fig. 2(a), in Fig. 2(b) the annealing temperature is changed and the other parameters are fixed. In this case, the PL peak energy is changed in a smaller energy range, i.e., from 1.41 to 1.30 eV, corresponding to the size change of 4.2–5.2 nm. Although the change in size is smaller than that in Fig. 2(a), the variation of the delay time is much larger. It is clear that a higher annealing temperature results in a longer PL delay, even if the size of nc-Si, i.e., the PL peak energy, is the same. Therefore, in addition to a size, there exists another parameter that affects the energy transfer rate.

In order to discuss this in more detail, we quantitatively analyze the observed data. In the present Er and nc-Si concentration range, we can assume that one nanocrystal interacts with one  $\text{Er}^{3+}$ . Under this assumption, in the simplest model,  $\text{Er}^{3+}$  PL intensity is expressed as

$$I(t) \propto \exp(-w_{\text{Er}}t) - \exp[-(w_{\text{Tr}} + w_{\text{Si}})t], \quad (1)$$

where  $w_{\text{Si}}$ ,  $w_{\text{Er}}$ , and  $w_{\text{Tr}}$  are the recombination rates of excitons in nc-Si and  $\text{Er}^{3+}$ , and the energy transfer rate, respectively. In this equation, both the rising and decaying parts of the curves are expressed with a single exponential function. However, as can be seen in Fig. 2(b), the intensity rises very fast until reaching about 70% of the maximum intensity and then starts to rise slowly. This behavior is apparently different from Eq. (1).

To reproduce the observed decay curves, we have to consider at least two different energy transfer processes occurring simultaneously; one process is faster than our time resolution (100 ns), and the other is slower and depends strongly on the samples. We define the number of  $\text{Er}^{3+}$  ions which interact very strongly with nc-Si and contribute to the fast process as  $N_{\text{Er}}^f$ , and the number of  $\text{Er}^{3+}$  ions which interact weakly and contribute to the slow process as  $N_{\text{Er}}^s$ . The energy transfer rate of each process is  $w_{\text{Tr}}^f$  and  $w_{\text{Tr}}^s$ , respectively. Under the assumption that one nanocrystal interacts with one  $\text{Er}^{3+}$ ,  $N_{\text{Er}}^f$  is equal to the number of nc-Si interacting strongly with  $\text{Er}^{3+}$  ( $N_{\text{Si}}^f$ ), and  $N_{\text{Er}}^s$  is equal to those weakly interacting with  $\text{Er}^{3+}$  ( $N_{\text{Si}}^s$ ). After pulsed excitation, the number of excited nc-Si that can transfer energy to  $\text{Er}^{3+}$  is

$$N_{\text{Si}}(t) = N_{\text{Si}_0}^f \exp[-(w_{\text{Tr}}^f + w_{\text{Si}})t] + N_{\text{Si}_0}^s \exp[-(w_{\text{Tr}}^s + w_{\text{Si}})t], \quad (2)$$

where  $w_{\text{Si}}$  is the recombination rate of excitons in nc-Si, and  $N_{\text{Si}_0}^f$  and  $N_{\text{Si}_0}^s$  denote the number of nc-Si excited at  $t=0$ . If we ignore direct excitation of  $\text{Er}^{3+}$ , the excitation rate of  $\text{Er}^{3+}$  can be

$$G(t) = w_{\text{Tr}}^f N_{\text{Si}_0}^f \exp[-(w_{\text{Tr}}^f + w_{\text{Si}})t] + w_{\text{Tr}}^s N_{\text{Si}_0}^s \exp[-(w_{\text{Tr}}^s + w_{\text{Si}})t], \quad (3)$$

TABLE I. List of samples studied in this work. Er concentration is fixed to 0.11 at. % for all the samples. Recombination rates of nc-Si ( $w_{Si}$ ) and Er ( $w_{Er}$ ) are obtained from PL decay curves. The ratio of slow to fast energy transfer processes ( $N_{Er}^s/N_{Er}^f$ ) and the energy transfer rate of the slow process ( $w_{Tr}^s$ ) are obtained by fitting experimental decay curves to a model.  $w_{Tr}^{s*}$  is obtained by subtracting the time necessary for  $Er^{3+}$  to relax from higher excited states to the first excited state from  $1/w_{Tr}^s$  (see Ref. 23).

Ta (°C)	Si (vol %)	PL peak energy (eV)	$w_{Si}$ (s <sup>-1</sup> )	$w_{Er}$ (s <sup>-1</sup> )	$N_{Er}^s/N_{Er}^f$	$w_{Tr}^s$ (10 <sup>3</sup> s <sup>-1</sup> )	$w_{Tr}^{s*}$ (10 <sup>3</sup> s <sup>-1</sup> )
1150	2.43	1.52	8692	255	0.80	191	366
1200	2.43	1.43	5931	165	0.64	42.4	47.4
1250	2.43	1.35	3927	125	0.53	14.4	14.9
1100	4.08	1.52	11515	291	0.76	265	785
1150	4.08	1.46	7795	318	0.62	176	314
1200	4.08	1.37	5061	184	0.53	49.7	56.8
1250	4.08	1.35	3927	173	0.30	17.6	18.4
1100	6.66	1.46	10870	367	0.81	269	821
1150	6.66	1.40	6897	320	0.58	139	213
1200	6.66	1.36	4916	178	0.49	35.2	38.6
1250	6.66	1.33	3631	163	0.34	21.2	22.4
1100	9.28	1.41	10322	447	0.51	222	499
1150	9.28	1.38	6598	305	0.47	96.4	127
1200	9.28	1.31	4191	189	0.50	24.6	26.2
1250	9.28	1.30	3188	199	0.40	17.1	17.9
1100	11.1	1.35	9688	465	0.37	130	193
1150	11.1	1.36	6299	318	0.42	70.5	85.6
1200	11.1	1.34	4626	254	0.37	38.8	43.0
1250	11.1	1.30	3188	248	0.37	18.2	19.1

and the number of  $Er^{3+}$  ions in the excited state is

$$N_{Er}(t) = \frac{w_{Tr}^f N_{Si_0}^f}{w_{Tr}^f + w_{Si} - w_{Er}} \{ \exp(-w_{Er}t) - \exp[-(w_{Tr}^f + w_{Si})t] \} + \frac{w_{Tr}^s N_{Si_0}^s}{w_{Tr}^s + w_{Si} - w_{Er}} \times \{ \exp(-w_{Er}t) - \exp[-(w_{Tr}^s + w_{Si})t] \}. \quad (4)$$

As can be seen in Fig. 2(b), the fast process is faster than our time resolution, and is also faster than the lifetimes of nc-Si PL (100  $\mu$ s–1 ms) and  $Er^{3+}$  PL ( $\sim$ 5 ms). Therefore, Eq. (4) can be approximated as

$$N_{Er}(t) = N_{Si_0}^s \left\{ \left( \frac{N_{Si_0}^f}{N_{Si_0}^s} + \frac{w_{Tr}^s}{w_{Tr}^s + w_{Si} - w_{Er}} \right) \exp(-w_{Er}t) - \frac{w_{Tr}^s}{w_{Tr}^s + w_{Si} - w_{Er}} \exp[-(w_{Tr}^s + w_{Si})t] \right\}. \quad (5)$$

Equation (5) multiplied by  $w_{Er}$  results in the PL intensity. Since the excitation rate of nc-Si does not depend on whether the energy transfer is fast or slow,  $N_{Si_0}^f/N_{Si_0}^s = N_{Si}^f/N_{Si}^s$ , and from the assumption that one nanocrystal interacts with one  $Er^{3+}$ ,  $N_{Si}^f/N_{Si}^s = N_{Er}^f/N_{Er}^s$ . Therefore, PL intensity will be

$$I(t) \propto \left( \frac{N_{Er}^f}{N_{Er}^s} + \frac{w_{Tr}^s}{w_{Tr}^s + w_{Si} - w_{Er}} \right) \exp(-w_{Er}t) - \frac{w_{Tr}^s}{w_{Tr}^s + w_{Si} - w_{Er}} \exp[-(w_{Tr}^s + w_{Si})t]. \quad (6)$$

In Eq. (6),  $N_{Er}^f/N_{Er}^s$  and  $w_{Tr}^s$  are unknown parameters and  $w_{Er}$  and  $w_{Si}$  can be obtained experimentally from the decay curves of  $Er^{3+}$  and nc-Si PL. The decay time of nc-Si PL was obtained by fitting the tail part of the decay curves with a single exponential function. By using  $N_{Er}^f/N_{Er}^s$  and  $w_{Tr}^s$  as fitting parameters, we fitted all of the experimental curves and extracted the values. The solid curves in Fig. 2 are the results of the fitting. The model can reproduce all the observed data with very good accuracy. The parameters used for and obtained from the fittings are summarized in Table I.

### B. Ratio of slow to fast energy transfer processes

In Fig. 3, the ratio of slow to fast energy transfer processes ( $N_{Er}^s/N_{Er}^f$ ) is plotted as a function of the peak energy of nc-Si PL. Since the PL spectrum of nc-Si is determined by its size distribution, the abscissa of Fig. 3 can be converted to the average size of nc-Si. We can see a good correlation between the two parameters, allowing us to conclude that  $N_{Er}^s/N_{Er}^f$  is the function of nc-Si size. In Fig. 3, in all the PL peak energy ranges studied,  $N_{Er}^s/N_{Er}^f$  is smaller than 1, indicating that the fast energy transfer process always dominates the whole energy transfer process. The straight line in Fig. 3

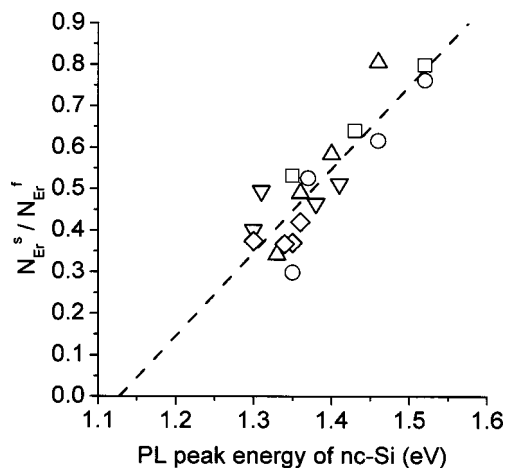


FIG. 3. The ratio of slow to fast processes estimated from curve fittings as a function of luminescence peak energy of Si nanocrystals. The dashed line is the result of least-squares fitting of the data. Excess Si concentrations are 2.43 (□), 4.08 (○), 6.66 (△), 9.28 (▽), and 11.1 vol % (◇).

is obtained by the least-squares fitting of all the data. The intercept of the line to the  $x$  axis is about 1.13 eV, which is very close to the band gap energy of bulk Si crystals. Although this coincidence might be accidental, it is clear that, for the samples consisting of very large nc-Si, only the fast energy transfer process occurs, suggesting that the fast transfer process is a direct inheritance of the process in bulk-Si:Er systems, and the slow process is a characteristic process occurring only in nc-Si:Er systems.

### C. Fast energy transfer process

In the above model, the energy transfer time includes pure energy transfer time and the time necessary for excited  $\text{Er}^{3+}$  to relax to the first excited state ( $\sim 2.5 \mu\text{s}$ ),<sup>23</sup> if it is excited to higher excited states. The transfer time of the fast process, which is shorter than our time resolution, is much shorter than the relaxation time. This suggests that the energy transfer is made only to the first excited state of  $\text{Er}^{3+}$  ( ${}^4I_{13/2}$ ), independent of the size of the nanocrystals.

The fact that the energy transfer is made to the first excited state despite the enlargement of the band gap of nc-Si supports the above conclusion that the fast energy transfer process is bulk-Si:Er-like, i.e., a trap-mediated energy transfer. In bulk-Si:Er systems, energy transfer is considered to be mediated by Er-related trap levels at about 150 meV below the conduction band of nc-Si; excitons are trapped at that level and the recombination energy of excitons is transferred to  $\text{Er}^{3+}$  by an Auger-like process.<sup>24,25</sup>

In general, the energy levels of localized states in nc-Si are not strongly modified by quantum size effects because they are localized in space.<sup>26,27</sup> In fact, the size-dependent shift of the dangling-bond-related PL of nc-Si observed at low temperatures is about half of that of the exciton PL, suggesting that the trap level is almost unaffected by size and the observed small shift reflects that of either a conduction or valence band edge.<sup>2,28–30</sup> Similarly, the energy of the Er-related trap level measured from the vacuum level is not expected to be strongly affected by the quantum size effects.

As a result, the energy of excitons trapped at Er-related centers will not be high enough to excite  $\text{Er}^{3+}$  to higher excited states, and the energy transfer is made only to the first excited state of  $\text{Er}^{3+}$ .

In bulk-Si:Er systems, dissociation of excitons from Er-related trap levels and energy back-transfer from excited  $\text{Er}^{3+}$  to the level is considered to be responsible for the observed strong temperature quenching of the PL. Both quenching processes require absorption of phonons to meet the energy conservation rule. In nc-Si:Er systems, even if the Er-related trap levels are not strongly affected by size, both conduction and valence band edges are shifted to higher and lower energies. These shifts prevent the dissociation of excitons, and also slightly increase the energy of the trapped excitons, although it is not high enough to excite the second excited state of  $\text{Er}^{3+}$ , resulting in very small temperature quenching.

### D. Slow energy transfer process

As the size decreases, the contribution of the slow energy transfer process becomes important, suggesting that the process is a characteristic one in nc-Si:Er systems. Furthermore, considering the very small energy transfer rate of this process, Er-related centers are not expected to be involved and excitons may interact directly with  $\text{Er}^{3+}$ .

If excitons in nc-Si directly interact with  $\text{Er}^{3+}$ , the energy transfer should be made mainly to higher excited states of  $\text{Er}^{3+}$  because the nc-Si PL peak energy in the present samples is always above 1.26 eV. The evidence that  $\text{Er}^{3+}$  is excited to higher excited states is obtained in the PL spectra of nc-Si, which are partially quenched due to the energy transfer to  $\text{Er}^{3+}$ .<sup>14</sup> At room temperature, by doping Er, nc-Si PL is quenched without changing its spectral shape very much and the spectra are featureless (Fig. 1). On the other hand, at low temperatures, periodic features can clearly be distinguished, i.e., the spectra are periodically suppressed, and dips appear periodically. In particular, energy higher than the third excited state of  $\text{Er}^{3+}$  ( ${}^4I_{9/2}$ ) is strongly suppressed. Periodic features appear at about the energies of the second ( ${}^4I_{11/2}$ ) and third ( ${}^4I_{9/2}$ ) excited states of  $\text{Er}^{3+}$  measured from the ground state, and the separation between the features is about 63 meV.

Since the energy levels of the  $\text{Er}^{3+}$  4*f* shell are discrete, only nc-Si with specific band gap energies can transfer energy resonantly; the energy transfer rate is the highest at the resonant energy. At other energies, phonons should be emitted in nc-Si to meet the energy conservation rule. This process is the most probable for phonons having the highest density of states, which in bulk Si are transverse optical phonons almost at the center of the Brillouin zone with an energy of 63 meV. If the band gap energy of nc-Si does not coincide with the excitation energy of  $\text{Er}^{3+}$  plus an integer number of the energy of those phonons, additional emission of acoustic phonons is required to conserve energy. This process has a smaller probability and the efficiency of the energy transfer is reduced. Consequently, equidistant features can be seen in quenched spectra that validate the phonon-assisted energy transfer. It is worth noting that, although the

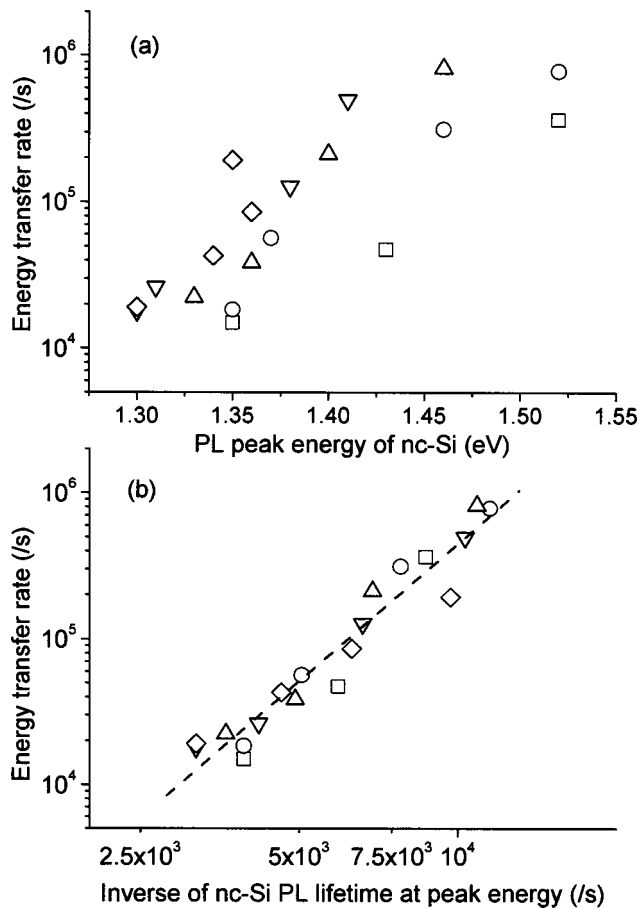


FIG. 4. Energy transfer rate of slow process is plotted as a function of (a) PL peak energy of nc-Si, i.e., the size of nc-Si, and (b) inverse of PL lifetime of nc-Si at PL peak energy, i.e., average exciton recombination rate in nc-Si. Excess Si concentrations are 2.43 (□), 4.08 (○), 6.66 (△), 9.28 (▽), and 11.1 vol % (◇). In the same symbols, higher-annealing temperature results in lower PL peak energy and smaller exciton recombination rate.

energy transfer rate is larger for some specific energies than others, energy transfer is possible in all energy ranges above 0.81 eV by emitting a series of phonons during the process. Very similar but more distinct PL features have been observed in nc-Si on which oxygen molecules are adsorbed.<sup>3,4</sup>

If the energy transfer is made to higher excited states, the energy transfer time we estimated includes the time for excited Er<sup>3+</sup> to relax to the first excited state. In order to extract only the time necessary to transfer energy, we subtract the relaxation time (2.5 μs; from <sup>4</sup>I<sub>11/2</sub> to <sup>4</sup>I<sub>13/2</sub> state)<sup>23</sup> from 1/w<sub>Tr</sub><sup>s\*</sup> and obtained 1/w<sub>Tr</sub><sup>s\*</sup>. The relaxation time from further higher states, e.g., <sup>4</sup>I<sub>9/2</sub>–<sup>4</sup>I<sub>11/2</sub> is considered to be much faster and negligible. The estimated values of w<sub>Tr</sub><sup>s\*</sup> are summarized in Table I.

First, we plotted 1/w<sub>Tr</sub><sup>s\*</sup> as a function of the nc-Si PL peak energy [Fig. 4(a)]. The energy transfer rate increases with increasing PL energy, i.e., with the decreasing size of nanocrystals. However, the data are largely scattered, and there seems to be another factor that also strongly affects the energy transfer rate. Among the largely scattered data, we can find a tendency. By comparing the energy transfer rates of the samples exhibiting a PL peak at nearly the same en-

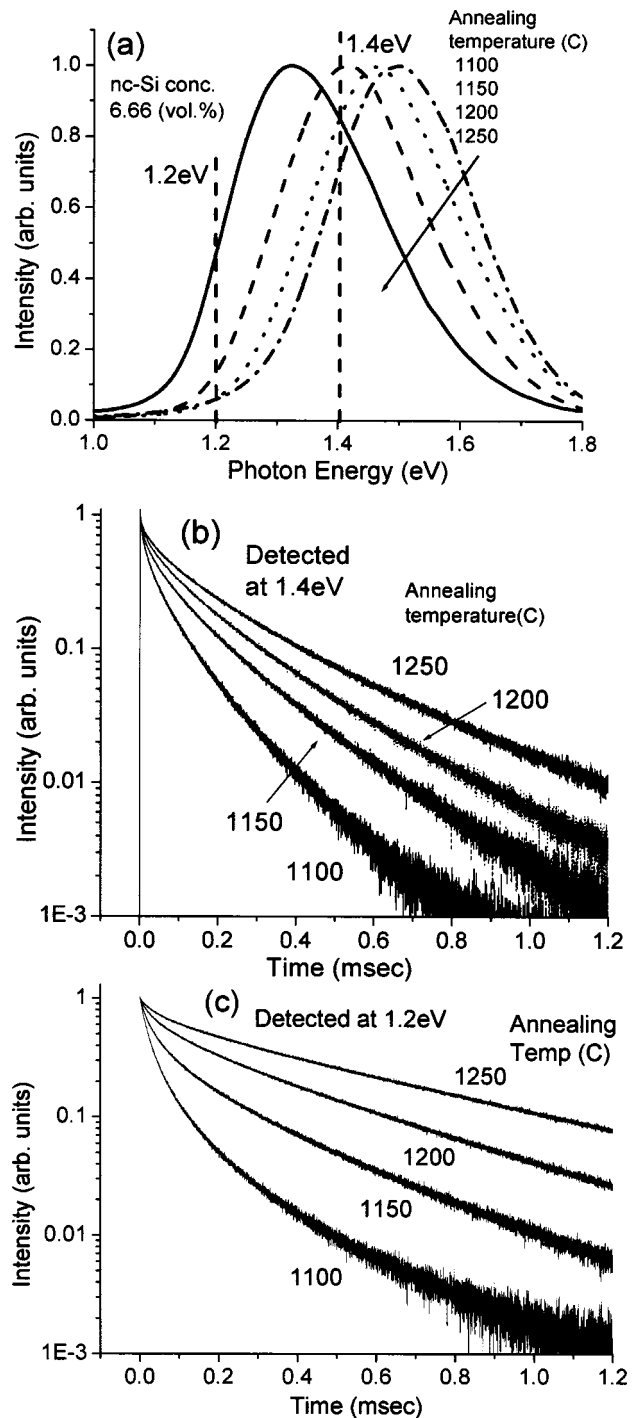


FIG. 5. (a) PL spectra of nc-Si prepared at different annealing temperatures and fixed excess Si concentration. PL decay curves detected at (b) 1.4 and (c) 1.2 eV for the same samples in (a).

ergy, the energy transfer rate is smaller for the samples annealed at higher temperatures (see Table I).

### E. Quality of nc-Si

To understand the implication of the data of Fig. 4, we will consider the “quality” of nc-Si. The word quality is rather ambiguous. However, it is sometimes useful to distinguish nc-Si grown from Si suboxide by annealing. Figure 5 shows one of the examples. In Fig. 5(a), PL spectra of pure

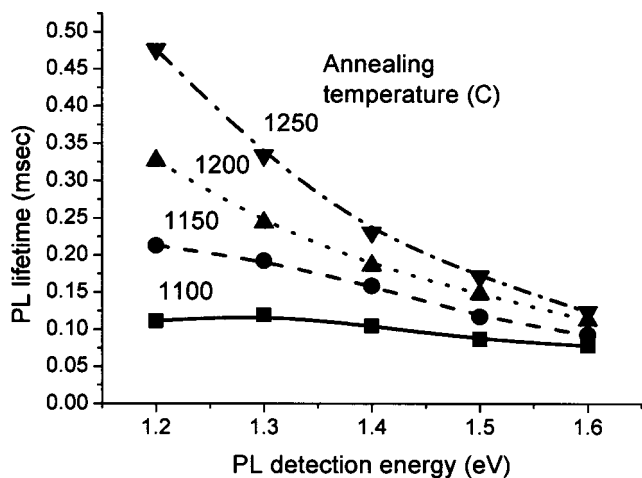


FIG. 6. PL lifetime vs detection energy for four nc-Si samples annealed at different temperatures.

nc-Si in  $\text{SiO}_2$  prepared with different annealing temperatures are plotted. The excess Si concentration is fixed for all samples. We can see that higher temperature annealing results in a lower energy shift of the PL. This shift is due to the increase in size. In addition to the peak shift, the annealing temperature affects the quality of the nanocrystals. In Figs. 5(b) and 5(c), PL decay curves measured at 1.4 and 1.2 eV are plotted. If the PL lifetime is determined only by size, the decay curve obtained at the same energy should be the same for all samples. However, the observed lifetime depends strongly on the annealing temperatures, and becomes longer at higher annealing temperatures. Furthermore, the shape of the decay curves depends strongly on the annealing temperatures. The decay curves of the samples annealed at higher temperatures are nearly a single exponential function, but those at lower temperatures largely deviated from the function. In Fig. 6, PL lifetimes obtained for four samples prepared with different annealing temperatures are plotted as a function of the PL detection energy. In low-temperature annealed samples, the PL lifetime is almost independent of the detection energy, while in high-temperature annealed samples, it depends heavily on the detection energy. In a quantum confinement model, the lifetime should depend heavily on the detection energy, because stronger confinement of excitons results in the enhancement of oscillator strength as well as the higher energy shift of the band gap. Therefore, higher-temperature annealed samples obey the prediction of the quantum size effects, and in this sense are high quality.

The different quality in samples annealed at different temperatures can be proved by resonant PL measurements. The PL spectra of nc-Si assemblies are always featureless and broad, if they are excited by blue or green light, because of the inhomogeneous broadening caused by size distribution. The size distribution can be lifted if the PL is excited in the low-energy tail of the luminescence band. In this method, only a small portion of nc-Si in the size distribution is excited, and a nearly homogenous spectrum can be obtained. In porous Si, with this method, PL peaks corresponding to the emission of momentum-conserving phonons can be ob-

served, and from the ratio of the phonon-assisted and non-phonon PL bands, the degree of the breakdown of the momentum conservation rule has been estimated.<sup>1</sup>

The same technique can be applied to synthesized nc-Si. In the resonant PL studies of the present samples, we found that higher-temperature annealed samples show clearer phonon-related structures, indicating that the indirect band gap character of bulk Si is held. On the other hand, in lower-temperature annealed samples, the nonphonon PL band was dominant and phonon structures were ill-defined, although the spectral shape under nonresonant excitation was nearly the same. This result implies that in low-temperature annealed samples, the translational symmetry of the crystal lattice is broken not only by the size effect but also by the disorder remaining in or on the surface of the nanocrystals, making the quasidirect optical transition more probable. This explanation is consistent with the shorter PL lifetime observed for lower-temperature annealed samples (Fig. 6). The simultaneous occurrence of the smearing of phonon-related structures in resonant PL spectra and the shortening of PL lifetimes was observed by doping germanium (Ge) in nc-Si ( $\text{Si}_{1-x}\text{Ge}_x$  alloy nanocrystals).<sup>31</sup> Breakdown of the translational symmetry by randomly substituting Si with Ge is considered to be responsible for the observed effects.

It is important to note here that low quality nc-Si means that bulk Si character is more smeared and the PL properties cannot be explained by a simple quantum size effect. It does not always mean lower PL quantum efficiency. In fact, in the present samples, PL intensity is not the highest for the samples annealed at 1250 °C, although the quality is the highest. Therefore, in nc-Si samples, one possible approach to obtaining higher quantum efficiency may be to introduce proper disorder if it does not lead to the formation of nonradiative recombination channels.

The other possible explanation of the data in Figs. 5 and 6 is that the strength of particle–particle interaction is changed by annealing temperature.<sup>15</sup> The interaction between nc-Si results in an energy transfer from smaller towards larger nc-Si, leading to a deviation of the decay curves from a single-exponential function and a redshift of the PL peak.<sup>15</sup> In this model, the deviation should be larger if we detect the PL at the higher-energy part of the PL spectra, because the energy transfer is made only from smaller to larger particles. However, as can be seen in Fig. 5(c), the deviation becomes larger for lower-temperature annealed samples, despite the fact that PL detection is made further from the PL peak energy for lower-temperature annealed samples. Furthermore, in our samples, the PL lifetime does not strongly depend on the fraction of excess Si, as can be found by comparing  $w_{\text{Si}}$  of samples with different excess Si and the same annealing temperature in Table I. These are evidences that different PL decay properties observed for samples annealed at different temperatures are not due to the change of the degree of particle–particle interactions, but reflect changes of the quality of individual nc-Si.

## F. What is the factor determining the energy transfer rate of the slow process

As can be seen in Fig. 6, the PL lifetime of nc-Si depends both on the size and quality of nc-Si. The PL lifetime obtained at a nc-Si PL peak energy contains information of both size distribution and quality. In Fig. 4(b), the energy transfer rate of the slow process ( $w_s^*$ ) is plotted as a function of the inverse of nc-Si PL lifetime, i.e., the recombination rate of excitons in nc-Si ( $w_{Si}$ ). In contrast to the plot as a function of PL peak energy shown in Fig. 4(a), the correlation is very good. It should be stressed that the energy transfer rate (ordinate) is estimated from the fitting of the observed PL decay curves of Er-doped samples, while the exciton recombination rate (abscissa) is obtained from the exciton PL of pure nc-Si samples prepared with the same excess Si concentration and annealing temperature of the Er-doped samples. From Figs. 4(a) and 4(b), we can conclude that the energy transfer rate of the slow process is determined by the recombination rate of excitons in nc-Si, and the reduction of size is just one approach to realizing a larger recombination rate of excitons.

The recombination rate of excitons in nc-Si exhibits strong temperature dependence.<sup>1,2</sup> At low temperatures excitons are populated in optically inactive spin-triplet states, which are several milli-electron-volts lower in energy than optically allowed spin-singlet states. The lifetime of the triplet states is 5–10 ms, which is almost independent of the size of nc-Si. On the other hand, at high temperatures, both states are nearly equally populated and the recombination rate is determined by the lifetime of the singlet state. The lifetime of the singlet state is between 1 ms to several microseconds, depending on the size of nc-Si. In the size range of the present samples, the recombination rate changes more than one order of magnitude from room temperature to liquid helium temperature, indicating that the energy transfer rate will be drastically reduced at very low temperatures. Unfortunately, we did not succeed in experimentally proving this phenomena. One of the obstacles is a defect-related infrared emission from nc-Si that is always observed for almost all kinds of nc-Si samples at low temperatures.<sup>2,28–30</sup> The lifetime of the emission is on the order of microseconds. Therefore, even if the intensity of the defect-related PL under cw excitation is very small, under pulsed excitation, the intensity just after excitation is much larger than that of Er<sup>3+</sup> PL, completely covering the time range we are interested in, i.e., the rising part.

It is important to note that, although the energy transfer rate of the slow process is expected to be decreased at low temperatures, energy transfer efficiency will not depend strongly on temperature because the smaller energy transfer rate will be compensated by the smaller radiative recombination rate of excitons [ $w_{Tr}(T)/w_{Si}(T) \approx \text{constant}$ ]. In fact, the intensity ratio of Er<sup>3+</sup> PL and nc-Si PL does not strongly depend on temperature.

Up to now, we avoided discussing how the fast and the slow processes are related to the sites of Er<sup>3+</sup>. Unfortunately, we have no clear clue for discussing this point. However, the observed strong size dependence of the ratio of the

two processes suggests that the bulk-Si:Er-like very fast energy transfer process is related to Er<sup>3+</sup> that stays in or very close to nc-Si because it is necessary to form an Er-related level in the band gap of nc-Si. On the other hand, the slow process comes from Er<sup>3+</sup> that is more separated from nc-Si. One of the promising methods to identify the sites responsible for the fast and slow processes is site-selective x-ray absorption spectroscopy. This method has been successfully applied to Er-doped Si thin films.<sup>32,33</sup> By applying the method to the two extreme samples with the largest and smallest sizes of nc-Si, it may be possible to identify independently the sites responsible for the fast and slow processes.

## IV. CONCLUSION

By analyzing the time transient of PL from Er<sup>3+</sup> doped into SiO<sub>2</sub> films containing nc-Si, two energy transfer processes (fast and slow processes) were found to coexist in each sample. The ratio of the two processes exhibited a clear dependence on the PL peak energy of Si nanocrystals, indicating that the ratio depends on the size of the nc-Si sensitizer. The observed size dependence suggests that the fast process is the direct inheritance of the process in bulk Si:Er systems, and the slow process is a characteristic process occurring only in nc-Si:Er systems. The energy transfer rate of the slow process was found to depend on the exciton recombination rate in nc-Si. Therefore, we can conclude that, in order to realize a higher energy transfer rate, the exciton recombination rate in nc-Si should be enhanced. This can be achieved by breaking down the translational symmetry of crystal lattices by reducing the size of nc-Si or by introducing disorder.

The present results imply that, from the point of view of application as an amplifier and a light-emitting device, perfect nc-Si that possess the indirect band gap character of bulk Si crystals is not suitable. Defective nc-Si:Er systems such as silicon-rich silicon dioxide, in which Si clusters smaller than 2 nm in diameter are considered to be dispersed, are more suitable. This conclusion is already empirically known and many reports concerning the application of similar systems utilize defective nc-Si assemblies.<sup>19–21</sup>

## ACKNOWLEDGMENTS

This work is supported by a Grant-in-Aid for Scientific Research from the Ministry of Education, Culture, Sports, Science and Technology, Japan, and in part by the Industrial Technology Research Grant Program in 2002 from the New Energy and Industrial Technology Development Organization (NEDO), Japan.

<sup>1</sup>D. Kovalev, H. Heckler, G. Polisski, and F. Koch, *Phys. Status Solidi B* **215**, 871 (1999).

<sup>2</sup>S. Takeoka, M. Fujii, and S. Hayashi, *Phys. Rev. B* **62**, 16820 (2000).

<sup>3</sup>D. Kovalev, E. Gross, N. Künzner, F. Koch, V. Yu. Timoshenko, and M. Fujii, *Phys. Rev. Lett.* **89**, 137401 (2002).

<sup>4</sup>E. Gross, D. Kovalev, N. Künzner, F. Koch, V. Yu. Timoshenko, and M. Fujii, *Phys. Rev. B* **68**, 115405 (2003).

<sup>5</sup>A. J. Kenyon, P. F. Trwoga, M. Federighi, and C. W. Pitt, *J. Phys.: Condens. Matter* **6**, L319 (1994).

<sup>6</sup>M. Fujii, M. Yoshida, Y. Kanzawa, S. Hayashi, and K. Yamamoto, *Appl. Phys. Lett.* **71**, 1198 (1997).

- <sup>7</sup>M. Fujii, M. Yoshida, S. Hayashi, and K. Yamamoto, *J. Appl. Phys.* **84**, 4525 (1998).
- <sup>8</sup>G. Franzò, V. Vinciguerra, and F. Priolo, *Appl. Phys. A: Mater. Sci. Process.* **A69**, 3 (1999).
- <sup>9</sup>C. E. Chryssou, A. J. Kenyon, T. S. Iwayama, C. W. Pitt, and D. E. Hole, *Appl. Phys. Lett.* **75**, 2011 (1999).
- <sup>10</sup>A. J. Kenyon, C. E. Chryssou, and C. W. Pitt, *Appl. Phys. Lett.* **76**, 688 (2000).
- <sup>11</sup>J. H. Shin, S.-Y. Seo, S. Kim, and S. G. Bishop, *Appl. Phys. Lett.* **76**, 1999 (2000).
- <sup>12</sup>G. Franzò, D. Pacifici, V. Vinciguerra, F. Priolo, and F. Iacona, *Appl. Phys. Lett.* **76**, 2167 (2000).
- <sup>13</sup>P. G. Kik, M. L. Brongersma, and A. Polman, *Appl. Phys. Lett.* **76**, 2325 (2000).
- <sup>14</sup>K. Watanabe, M. Fujii, and S. Hayashi, *J. Appl. Phys.* **90**, 4761 (2001).
- <sup>15</sup>F. Priolo, G. Franzò, D. Pacifici, V. Vinciguerra, F. Iacona, and A. Irrera, *J. Appl. Phys.* **89**, 264 (2001).
- <sup>16</sup>D. Pacifici, G. Franzò, F. Priolo, F. Iacona, and L. D. Negro, *Phys. Rev. B* **67**, 245301 (2003).
- <sup>17</sup>M. Fujii, S. Hayashi, and K. Yamamoto, *Appl. Phys. Lett.* **73**, 3108 (1998).
- <sup>18</sup>K. Watanabe, H. Tamaoka, M. Fujii, and S. Hayashi, *J. Appl. Phys.* **92**, 4001 (2002).
- <sup>19</sup>H. Han, S. Seo, and J. Shin, *Appl. Phys. Lett.* **79**, 4568 (2001).
- <sup>20</sup>H. Han, S. Seo, J. Shin, and N. Park, *Appl. Phys. Lett.* **81**, 3720 (2002).
- <sup>21</sup>F. Iacona *et al.*, *Appl. Phys. Lett.* **81**, 3242 (2002).
- <sup>22</sup>M. E. Castagna, S. Coffa, M. Monaco, L. Caristia, A. Messina, R. Mangano, and C. Bongiorno, *Physica E (Amsterdam)* **16**, 547 (2003).
- <sup>23</sup>The relaxation time can be estimated from PL lifetime at 1.26 eV due to the  $^4I_{11/2} \rightarrow ^4I_{15/2}$  transition. The observed lifetime is about 2.5  $\mu\text{s}$  at room temperature [D. Pacifici, G. Franzò, F. Priolo, F. Iacona, and L. D. Negro, *Phys. Rev. B* **67**, 245301 (2003)]. This time is not pure radiative recombination time but mainly reflects the relaxation of  $\text{Er}^{3+}$  to the first excited state, indicating that relaxation from higher excited states to the first excited state takes at least 2.5  $\mu\text{s}$ .
- <sup>24</sup>A. Polman, *J. Appl. Phys.* **82**, 1 (1997).
- <sup>25</sup>M. Forcales, T. Gregorkiewicz, M. S. Bresler, O. B. Gusev, A. F. I. V. Bradley, and J.-P. R. Wells, *Phys. Rev. B* **67**, 085303 (2003).
- <sup>26</sup>C. Delerue, M. Lannoo, G. Allan, and E. Martin, *Thin Solid Films* **255**, 27 (1995).
- <sup>27</sup>G. Allan, C. Delerue, M. Lannoo, and E. Martin, *Phys. Rev. B* **52**, 11982 (1995).
- <sup>28</sup>Y. Mochizuki, M. Mizuta, Y. Ochiai, S. Matsui, and N. Ohkubo, *Phys. Rev. B* **46**, 12353 (1992).
- <sup>29</sup>B. K. Meyer, D. M. Hofmann, W. Stadler, V. Petrova-Koch, F. Koch, P. Omling, and P. Emanuelsson, *Appl. Phys. Lett.* **63**, 2120 (1993).
- <sup>30</sup>B. K. Meyer, D. M. Hofmann, W. Stadler, V. Petrova-Koch, F. Koch, P. Emanuelsson, and P. Omling, *J. Lumin.* **57**, 137 (1993).
- <sup>31</sup>M. Fujii, D. Kovalev, J. Diener, F. Koch, S. Takeoka, and S. Hayashi, *J. Appl. Phys.* **88**, 5772 (2000).
- <sup>32</sup>M. Ishii, Y. Tanaka, T. Ishikawa, S. Komuro, T. Morikawa, and Y. Aoyagi, *Appl. Phys. Lett.* **78**, 183 (2001).
- <sup>33</sup>M. Ishii, T. Ishikawa, T. Ueki, S. Komuro, T. Morikawa, Y. Aoyagi, and H. Oyanagi, *J. Appl. Phys.* **85**, 4024 (1999).